Shock Waves (2008) 18:281–290
DOI 10.1007/s00193-008-0162-x

ORIGINAL ARTICLE

Shock and detonation wave diffraction at a sudden expansion in gas–particle mixtures

A. V. Fedorov · T. A. Khmel · Yu. V. Kratova

Received: 26 September 2007 / Revised: 9 July 2008 / Accepted: 10 July 2008 / Published online: 29 July 2008

Abstract Numerical modeling of the propagation of shock and detonation waves is carried out in a duct with an abrupt expansion for a heterogeneous mixture of fine particles of aluminum and oxygen. A considerable difference from corresponding flows in pure gas is found. The influence of the size and mass loading of particles on the flow and shock wave structure behind the backward-facing step is determined. As in gaseous detonations, three types of scenarios of detonation development are obtained. Specific features of the flow structure are revealed such as deformation of the combustion front due to interaction between the relaxation zone and the vortex structure. The influence of particle size and channel width on detonation propagation is analyzed.

Keywords Shock waves · Detonation · Diffraction · Gas suspensions

PACS 47.40.-x · 47.40.-Rs · 47.55-Kf

Communicated by L. Bauwens.

This paper is based on work that was presented at the 21th International Colloquium on the Dynamics of Explosions and Reactive Systems, Poitiers, France, July 23–27, 2007.

A. V. Fedorov · T. A. Khmel (✉) · Y. V. Kratova
Khristianovich Institute of Theoretical and Applied Mechanics SB RAS, Institutskaya 4/1, 630090 Novosibirsk, Russia
e-mail: khmel@itam.nsc.ru

A. V. Fedorov
e-mail: fedorov@itam.nsc.ru

Y. V. Kratova
e-mail: yulia@itam.nsc.ru

1 Introduction

Diffraction of shock and detonation waves is one of the fundamental problems in gas dynamics and mechanics of multi-phase media. The diffraction of a shock or detonation wave at a sudden expansion of a planar channel is of special interest since such a configuration is typical of technological devices.

Investigation of the processes of diffraction of shock waves in gaseous mixtures [1–3] shows that the flow structure behind a backward-facing step is rather complex. Shock waves interact with the vortex and shear layer structure, resulting in various types of near-wall shock wave reflections, and possibly formation of a secondary shock wave and a pair of shock waves induced by the vortex. Some aspects of this phenomenon, determined both from experimental and numerical studies, have been presented in a detailed review [3]. The problem of shock-wave (SW) diffraction on a square corner was used as a test in numerical simulations of unsteady compressible gas flows [4], where a comparative analysis of experimental data and results predicted by various numerical techniques was performed.

The process of diffraction of shock waves in gas–particle mixtures is more complex than in gas mixtures. The flow pattern is characterized by the additional influence of the relaxation process, of velocities and temperatures, for both phases. The typical scales over which these relaxation processes extent depend upon the particle sizes. Due to these additional geometric scales, the flow in the neighbourhood of the corner is no longer self-similar, unlike in the gas flow. Thus, analysis of the flow in a gas–particle suspension behind a step, resulting from a shock wave moving through, is of fundamental theoretical interest. However these issues have not been adequately studied, and there is little information available in publications.

Wang et al. [5] solved the problem of propagation of a planar SW above a square cavity filled by a motionless gas suspension numerically. They found that the shock waves in the cavity become attenuated with increasing load factor of particles and transform into compression waves. The particle size has a significant effect on the flow character and the wave structure in the cavity. For a suspension of coarse particles (250 μm), the flow structure was demonstrated to approach that in gas mixtures (this is obvious: indeed the relaxation zones behind the SW are then longer than the size of the cavity, and the solution is determined by the frozen gas flow).

A similar problem for a trapezoid cavity was considered in [6] for a single particle (neglecting the effect of particles on the gas flow). It was shown that lifting of particles from the cavity walls is significantly affected by the SW strength, initial position of the particle, and its size. Motion of particles in the upstream direction (saltation) was observed, which can lead to stable accumulation of particles near the compression corner behind the step.

Detonation flows are also characterized by additional geometric scales, which are determined by chemical processes, such as combustion and the ignition delay (induction). It is pointed out in [7] that the chemical processes occurring in the detonation wave lead to a loss of self-similarity of the flow in gaseous mixtures unlike similar processes of shock-wave diffraction in inert media.

It is also known for gases that different values of the ratio of reaction zone length and the reference geometric parameter of the configuration can result in qualitatively different flow regimes. Following detonation failure behind a backward-facing step, a re-initiation is possible at the expense of the diffracted wave reflection from the wide channel wall, with a further merging of the shock wave and combustion front. Detailed flow patterns in such a regime, which agree well with experimental Schlieren photographs, were obtained in [8] by numerical modeling. Three regimes of detonation propagation resulting from diffraction of a planar detonation wave on a backward-facing step were identified by numerical simulation in [9]. These regimes were termed a subcritical one (complete detonation failure), critical one (a partial failure with re-initiation), and a supercritical one (continuous propagation). The switch from one regime to another was associated with the value of the activation energy (which causes also a variation of the reaction zone length). It was observed that a system of transverse waves could appear at the detonation front in one of the regimes.

Results of similar investigations for gas–particle mixtures are very scarce. The detonation propagation processes in mixtures of gas and monofuel particles in pipes with a sudden expansion were analyzed in [10]. The mass load of the mixture was found to significantly affect the value of critical diameter ratio for detonation failure prevention. However the detailed structure of the two-phase mixture flow was not presented, and the influence of the particle mass loading on the process was not studied. Detonation wave diffraction processes in a two-phase medium were studied numerically in [11] on a backward-facing step, including also a rectangular one. A powder-like explosive characterized by a high detonation speed (7600 m/s) was considered. Results showed flow patterns qualitatively similar to gaseous mixtures, although the authors determined the mean parameters of the mixture without identification of phases. Thus, the propagation of shock and detonation waves in heterogeneous media in regions of complex geometry was practically not investigated, especially the influence of relaxation processes of interphase interaction.

In the present work, we investigate numerically the processes of shock diffraction and detonation waves on the cross-sectional jump of a planar channel in mixtures of fine aluminum particles and oxygen. Since the gas phase does not contain any fuel, the detonation is due only to the heterogeneous reaction of oxidation of aluminum particles.

The purpose of the work is as follows:

- Investigation of the influence of gas–particle mixture parameters on the flow wave pattern at a diffraction of shock waves on a backward-facing rectangular step;
- Determination of the influence of particles size and of the channel geometry on the wave pattern and detonation flow at diffraction of detonation waves.

2 Problem formulation

The problem considers a flat duct with an abrupt expansion of the cross section, filled with a homogeneous mixture of oxygen and fine aluminum particles. The duct is assumed to be symmetric with respect to the x axis; therefore, it sufficient to consider its upper or bottom part (Fig. 1). A supported steady planar shock wave or self-sustained planar detonation wave followed by a rarefaction wave propagates along the duct in the gas–particle mixture. We investigate the passage of this wave from the narrow part of the duct to the wide part. Geometry is shown in Fig. 1. L_1 is the initial location of the

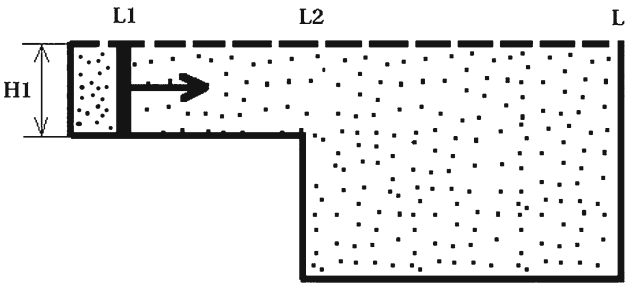

Fig. 1 Computational flow domain

wave front, L_2 is the length of the narrow part of the duct and $L$is the length of the computational domain. H_1 is the width the narrow part of the duct and H_2 is the width of the wide part, $H_2 \gg H_1$.

A mathematical model of detonation of aluminum particles in oxygen was developed in [12,13] and verified by comparison with experimental data [14]. The model is based upon the concept of a two-velocity two-temperature continuum of the mechanics of heterogeneous media. Aluminum combustion is described as a reduced reaction initiated after the particle achieves a critical temperature (the ignition temperature) that accounts for incomplete particle combustion (due to the oxide film growth). Parameter values (ignition temperature, activation energy, heat release, and chemical reaction velocities) were determined from experimental data, including detonation velocity, ignition zone length and combustion delay. The model reproduces experimental results [14] such as the effect of particle concentration on stationary detonation velocity. The characteristic time of aluminum particle combustion in oxygen agrees with the data presented in [15,16]. The ignition temperature value determining the induction time was set to be close to the value adopted in [17]. A theoretical analysis of steady detonation structure was carried out in [12,13,18]; the results computed for parameters in the Chapman—Jouguet plane agree with experimental data [14] also for pressure and concentration values of unburnt particles. In [19] the model was applied to computations of two-dimensional unsteady detonation flows, and it was used in [20] for numerical investigation of shock-wave initiation of detonation. The results of [20] agree with experimental and computed data of [17] on initiation energy values.

The flow in gas–particle mixtures is governed by Euler's equations, namely conservation of mass, momentum, and energy for each phase:

$$
\begin{aligned}
&\frac{\partial \rho_i}{\partial t} + \frac{\partial \rho_i u_i}{\partial x} + \frac{\partial \rho_i v_i}{\partial y} = (-1)^{\text{i-1}} J \\
&\frac{\partial \rho_i u_i}{\partial t} + \frac{\partial \left[\rho_i u_i^2 + (2-i)p\right]}{\partial x} + \frac{\partial \rho_i u_i v_i}{\partial y} \\
&\quad = (-1)^{\text{i-1}}(-f_x + J u_2) \\
&\frac{\partial \rho_i v_i}{\partial t} + \frac{\partial (\rho_i u_i v_i)}{\partial x} + \frac{\partial \left[\rho_i v_i^2 + (2-i)p\right]}{\partial y} \\
&\quad = (-1)^{\text{i-1}}(-f_y + J v_2) \\
&\frac{\partial \rho_i E_i}{\partial t} + \frac{\partial \left[\rho_i u_i (E_i + (2-i)p/\rho_1)\right]}{\partial x} \\
&\qquad + \frac{\partial \left[\rho_i v_i (E_i + (2-i)p/\rho_1)\right]}{\partial y} \\
&\quad = (-1)^{i-1}(-q - f_x u_2 - f_y v_2 + J E_2)
\end{aligned}
\tag{1}
$$

The model is closed by equations of state, allowing for the fact that the volume concentration of particles is small

$$
p = \rho_1 R T_1,\ E_i = (u_i^2 + v_i^2)/2 + c_{v,i} T_i + (i-1)Q, \tag{2}
$$

the laws of velocity and heat exchange between the phases

$$
\begin{aligned}
\bar{f} &= \frac{3 m_2 \rho_{11}}{4d} c_D \, |\bar{u}_1 - \bar{u}_2| \, (\bar{u}_1 - \bar{u}_2), \\
q &= \frac{6 m_2 \lambda_1}{d^2} Nu (T_1 - T_2),
\end{aligned}
\tag{3}
$$

and reduced chemical kinetics

$$
J = \frac{\rho}{\tau_\xi} \max(0, (\xi - \xi_k)) \exp(-E_a / R T_2) \text{ at } T_2 \geq T_{ign}; \tag{4}
$$

$J = 0$ at $T_2 < T_{\text{ign}}$ and in the problem of the SW diffraction in mixtures of gas and inert particles.

The interphase interaction processes are described by a correlation matched with experimental data on the trajectories of particles motion behind shock waves [21]. The approximation $Nu = 2 + 0.6 Re^{1/2} \Pr^{1/3}$ determines the Nusselt number as a function of the Reynolds number and the Prandtl number, and the formula

$$
\begin{aligned}
c_D(\text{Re}, M_{12}) = &\left(1 + \exp\left(-\frac{0,43}{M_{12}^{4.67}}\right)\right) \\
&\times \left(0,38 + \frac{24}{\text{Re}} + \frac{4}{\sqrt{\text{Re}}}\right)
\end{aligned}
\tag{5}
$$

is used for the drag coefficient, where the Reynolds and Prandtl numbers are defined as

$$
\text{Re} = \frac{\rho_{11} d \, |u_1 - u_2|}{\mu}, \quad M_{12} = \frac{|u_1 - u_2| \sqrt{\rho_{11}}}{\sqrt{\gamma_1 p}}.
$$

(The drag coefficient determined by formula (5) is shown by computations to differ little in detonation flows from the one determined by the known Henderson formula [22]).

In formulas (1)–(5), p is the pressure; ρ_i, u_i, v_i, T_i, E_i, and $c_{v,i}$ are the mean density, the longitudinal and transverse velocity components, the temperature, the total energy per unit mass, and the specific heat of the ith phase ($i = 1, 2$), respectively. The relative mass concentrations of gas (subscript 1) and particles (subscript 2) are defined as $\xi_i = \rho_i / \rho$, $\rho = \sum_i \rho_i$, $\rho_i = \rho_{ii} m_i$, where ρ_i and ρ_{ii} are the mean and true density of each phase, respectively, $\rho_{22} = const$, m_i is the volume concentration of the ith phase, ξ_k is the minimum particle fraction that is allowed (unburnt particles with condensed aluminum oxide), d is the particle diameter, c_D is the particle drag coefficient, λ_1 is the thermal conductivity of the gas, Re, Nu, Pr are the Reynolds, Nusselt, and Prandtl numbers, μ is the gas viscosity, γ_1 is the gas adiabatic exponent, E_a is the activation energy, T_{ign} is the ignition temperature, τ_ξ is the characteristic combustion time.

The initial values of the mixture properties were taken identical to those used in [18,19]: $p_0 = 1\,\text{atm}$, $T_0 = T_{20} = 300\,\text{K}$, $\Pr = 0.7$, $c_{v,1} = 914\,\text{J/(kg K)}$, $c_{v,2} = 880\,\text{J/(kg K)}$, $T_{ign} = 900\,\text{K}$, $E_a = 10^6\,\text{J/kg}$, $Q = 2,94 \cdot 10^6\,\text{J/kg}$, $\xi_0 = 0.55$, $\rho_{20} = 1.34\,\text{kg/m}^3$. The particle size was varied within

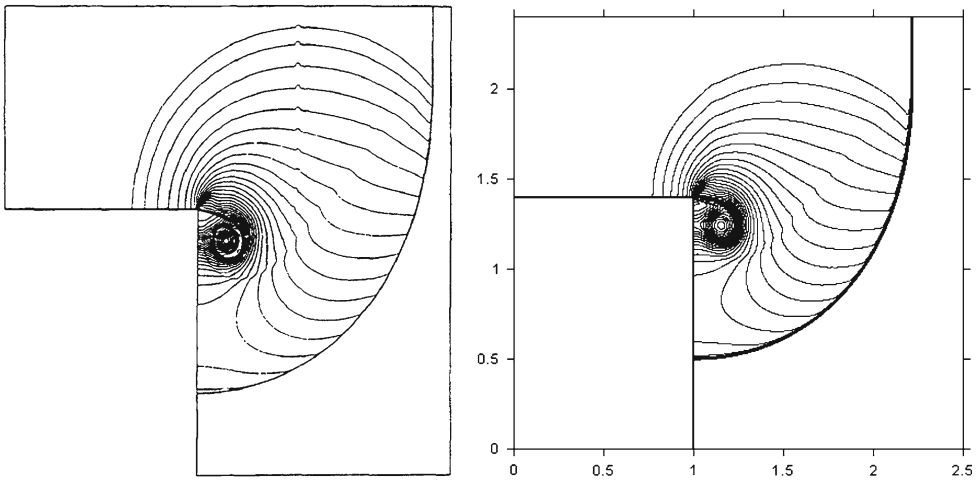

Fig. 2 Computed shock-wave diffraction pattern on a backward-facing step in air (gas density contours), $M = 1.5$: [4, calculations by M. Watanabe] (**a**), present calculations (**b**)

1–5 μm. For the constant determining the reaction rate of particle combustion, we use the formula $\tau_\xi = \tau_0\,(\mathrm{d}/\mathrm{d}_0)^2$ with $\tau_0 = 0.0024$ ms, $d_0 = 10$ μm, $E_\mathrm{a} = 10^6$ J/K in accordance to [19]. The quadratic dependence of combustion time on the particle diameter for combustion of aluminum in oxygen is confirmed by the data presented in [16]. The value τ_0 ensures agreement with the data in [15] on the duration of aluminum particle combustion in pure oxygen.

The system (1)–(5) is solved under the following initial conditions:

$$t = 0, \qquad \phi = \begin{cases} \phi_l, & 0 < x < L_1, \\ \phi_0, & L_1 < x \le L \end{cases}, \tag{6}$$

where $\phi = \{\rho_1, \rho_2, \rho_1 u_1, \rho_2 u_2, \rho_1 v_1, \rho_2 v_2, \rho_1 E_1, \rho_2 E_2\}$ is the solution vector, ϕ_l is the solution corresponding to a steady planar detonation wave, ϕ_0 is the initial state ahead of the front.

3 Computational method

The numerical method was tested on 1 upon-D and 2-D problems of detonation initiation and propagation in [23,24] and applied successfully in [19,25]. The method includes the Harten TVD scheme for the gaseous phase and the Gentry—Martin—Daly upwind difference scheme for the solid phase dynamics. For convenience of numerical implementation of the two-dimensional TVD scheme in the current geometry, a planar channel of maximum width is used as the computational domain. At each time step, the computation is performed in the entire region. Then the boundary conditions on the walls of both the narrow and wide parts of the channel are set as thermally insulated slip walls.

The conditions at the inlet (left) boundary are specified appropriately for the specific problem. Here, for the shock-wave diffraction problem, a supporting piston is specified (thus the left boundary condition corresponds to the values of the final equilibrium state behind the shock wave). In the detonation wave diffraction problem, the narrow channel is taken to be quite long. Near the left boundary the flow corresponding to the left end of the expansion wave is nearly one-dimensional and directed outside the domain ($u_{1,2} < 0$), which allows for outflow boundary conditions. The initial state is specified at the right boundary, and the computation is pursued until the front reaches this boundary.

A uniform two-dimensional finite-difference grid with a step corresponding to $2 \cdot 10^{-4}$ m, was used, which corresponds to approximately 20 points in the minimum relaxation scale (the zone of 1 μm diameter particle combustion). The influence of grid size on the solution was analyzed in [23,24]. Figure 2 shows the results of a test computation of the diffraction of a shock wave of strength M = 1.5 in a non-dusty gas (air) in the form of density contours. The current results in Fig. 2a are compared with flow patterns obtained by the Harten-Yee scheme [4, calculations by M. Watanabe] shown in Fig. 2b.

Results agree both in the general flow pattern and in features such as the shape of the curve corresponding to the diffracted shock wave front, the size and shape of the vortex zone, the inclination angle of the attached shock, etc. Thus, the test computation results for a non-dusty gas agree well with known computional results, which confirms that our code is suitable for the analysis of the SW diffraction process in a two-phase mixture.

4 Characteristic features of the SW diffraction in gas–particle mixtures

A specific feature of shocked flows in heterogeneous mixtures that distinguishes them from inviscid gas flows is that here the shock waves exhibit an internal structure caused by the processes of thermal and velocity relaxation of the phases. The typical relaxation process scales depend upon the particles size, and for monodisperse gas–particle mixtures

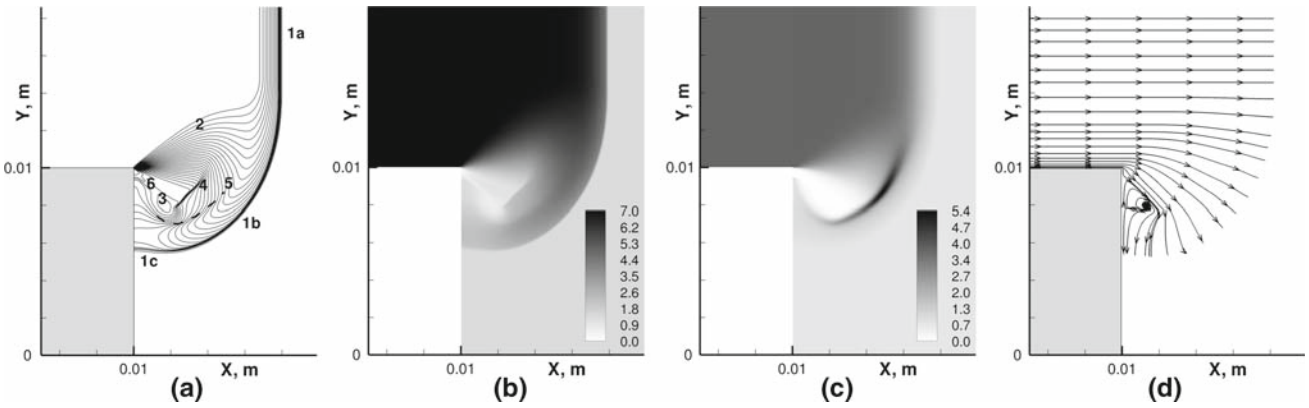

Fig. 3 Shock-wave diffraction on a backward-facing step in a gas—particle mixture, $M = 3$, $t = 0.16\,\mu s$: gas density contours (**a**), gas density field, kg/m3 (**b**), density fields of the dispersed phase, kg/m^3 (**c**), gas flow stream traces (**d**)

under consideration they are also comparable with the geometric scales (the duct transverse dimensions). The presence of these relaxation parameters may affect significantly both the SW diffraction pattern at the passage of the backward-facing step and further SW propagation in the duct.

Computational results for the flow forming at the SW diffraction around the expansion right angle for a mixture of particles 1 μm in diameter and a fixed initial loading $\rho_{2,0} = 0.69\,\text{kg/m}^3$ are presented in Fig. 3. The data presented are obtained for a Mach number M = 3 which provides a supersonic flow around the corner of the backward-facing step behind the SW. Figure 3a and b show the gas density field and contours. Figure 3c and d show the particle density field and gas flow stream traces.

Typical features of similar flow in gases, as presented in [1,2], are identified in Fig. 3a. The shock wave (1) includes three parts: incident shock (1a), diffracted shock (1b), and reflected shock with Mach stem (1c). An expansion fan (2) is formed in the neighborhood of the backward-facing step. The characteristics converge towards the corner point at a supersonic flow or trend to the duct wall in front of the corner point at a subsonic flow (Fig. 2). The flow behind the backward-facing step is characterized by the presence of a vortex (3), secondary shock (4), contact surface (dashed line 5), and attached shock (6). The contact surface and the secondary shock manifest themselves most clearly for high values of the Mach numbers (M > 2). The wave pattern is on the whole similar to that in a non-dusty gas, with vortex, secondary shock, and an expansion wave separating regions of different densities in Fig. 3b.

The effect of SW strength on the flow pattern behind the backward-facing step is similar to SW diffraction in gases [1,2]. An increase in the incident SW Mach number affects the shape of the regions corresponding to the fan of expansion waves and the vortex zone as well as the type of diffracted SW reflection from the backward-facing step wall.

The presence of particles affects considerably the form and dimensions of the typical flow structures. In particular, the contact discontinuity 5 is localized inside the region and does not reach the front. Besides, a shock wave in the mixture is followed by the relaxation zone, which reveals itself in particular by a transformation of shapes of the contours corresponding to the expansion fan.

An analysis of the particles density patterns (Fig. 3c) shows that an expansion zone with a very low content of particles (the mean density of particles being less than $0.05\,\text{kg/m}^3$) forms behind the backward-facing step. This is caused by the fact that immediately after the shock wave passes over the backward-facing step, the direction of the gas motion changes abruptly while the particles continue moving in the same direction due to their larger inertia. Thus, a zone exists behind the backward-facing step, which the particles do not reach as they flow from upstream. The particles initially present in this zone behind the backward-facing step follow the diffracted shock wave and escape from that region. The vortex gas flow (Fig. 3d) forming behind the backward-facing step contributes to a further separation of particles. Accumulation of particles occurs in a layer adhering to the contact surface, which may clearly be seen in Fig. 3c. Since the discrete phase (as well as the gas phase) velocity in the expansion fan is much higher than behind the diffracted SW (by virtue of its weakening behind the backward-facing step), the particles decelerate in a region behind the contact surface and the secondary shock. This results in a considerable concentration increase, the mean density of particles reaching a value of $5.36\,\text{kg/m}^3$, an increase of nearly an order of magnitude. Thus a peculiar kind of a ρ-layer appears, that is proper to the SW structures in gar-particle mixtures. It is worth emphasizing that in the current case, this particle layer occurs near the contact discontinuity.

Influence of the particles mass loading on the diffraction pattern is shown in Fig. 4. Pressure contours and numerical

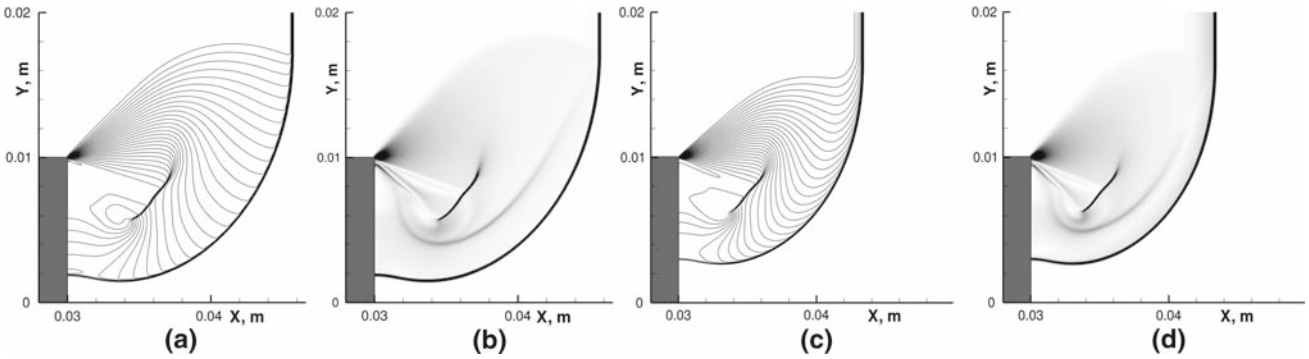

Fig. 4 Influence of the particles loading in the gas–particle mixture on flow pattern, pressure contours and numerical Schlieren pictures for the gaseous phase, $M = 3$, $d = 1\,\mu$m, $t = 30\,\mu$s: $\rho_{2,0} = 0.027\,\text{kg/m}^3$ (**a, b**), $\rho_{2,0} = 0.27\,\text{kg/m}^3$ (**c, d**)

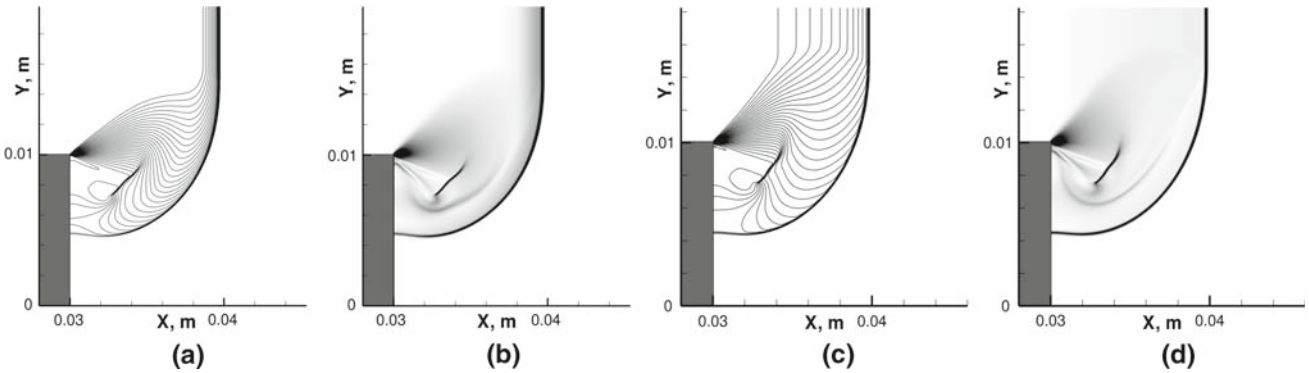

Fig. 5 Particles size influence on the wave pattern. Pressure contours and numerical Schlieren pictures of gaseous phase, $M = 3$, $\rho_2, 0 = 0.69\,\text{kg/m}^3$, $t = 34\,\mu$s, $d = 1\,\mu$m (**a, b**), $d = 3\,\mu$m (**c, d**)

schlieren images are presented for $d = 1\,\mu$m, $t = 30\,\mu$s and for two particle mass fraction values, $\rho_{2,0} = 0.027\,\text{kg/m}^3$ (*a*, *b*) and $\rho_{2,0} = 0.27\,\text{kg/m}^3$ (*c*, *d*). The variation of mass load of particles leads to an alteration of the equilibrium adiabatic exponent γ_e of the mixture hence different shock waves. Therefore, the SW location is different for the same moment in time in Fig. 4a, b, c, d. Besides, if for $\rho_{2,0} = 0.027\,\text{kg/m}^3$ (Fig. 4a, b) the pattern nearly coincides with the pattern in gases, for $\rho_{2,0} = 0.27\,\text{kg/m}^3$ (Fig. 4c, d), features characteristic of two-phase mixtures become noticeable. Effects related to the influence of relaxation zones include: bending of the expansion waves, different flow between the diffracted SW front and the contact discontinuity and flow in the vortex zone are revealed in Fig. 4c and d. In particular, as a result of the interaction of the fan of expansion waves with the relaxation zone, the gas density contours turn to the symmetry line in Fig. 4c rather than to the leading SW front in Fig. 4a. The contours are also strongly curved near the diffracted SW front and they merge with the front under very small angles. Thus, the influence of particles on the flow is substantial already at values of relative mass concentration of particles $\xi_2 = \rho_{2,0}/(\rho_{2,0}+\rho_{1,0})$ of the order of 0.1.

The characteristic lengths of relaxation zones depend on particle diameter. The influence of particles size on the diffracted SW structure in the mixture is shown in Fig. 5, where results are presented for $\text{M} = 3$, $\rho_{2,0} = 0.69\,\text{kg/m}^3$, $t = 34\,\mu$s, for two values of particle diameter: 1 μm (Fig. 5a, b) and 3 μm (Fig. 5c, d). It is seen from the comparison of the gas pressure contours (Fig. 5a, c) and numerical schlieren images (Fig. 5b, d) that an increase in particle diameter leads to a change in the inclination angle of the secondary shock so that the vortex region shape and the expansion fan shape change.

Since the relaxation zone scales depend upon particle size, and the scales of typical flow structures at the SW diffraction behind the backward-facing step (the diffracted SW, vortex zone, etc.) change with time, then for each particles size there exists a time interval in which the effect of the presence of a solid phase is maximum. This occurs when the scales of typical zones and the scales of relaxation zones are comparable. If relaxation scales are much larger than the structure of the diffracted wave (at small times) then the flow may be considered as a frozen particle flow. In the opposite case (at very large times) the flow may be considered as an equilibrium

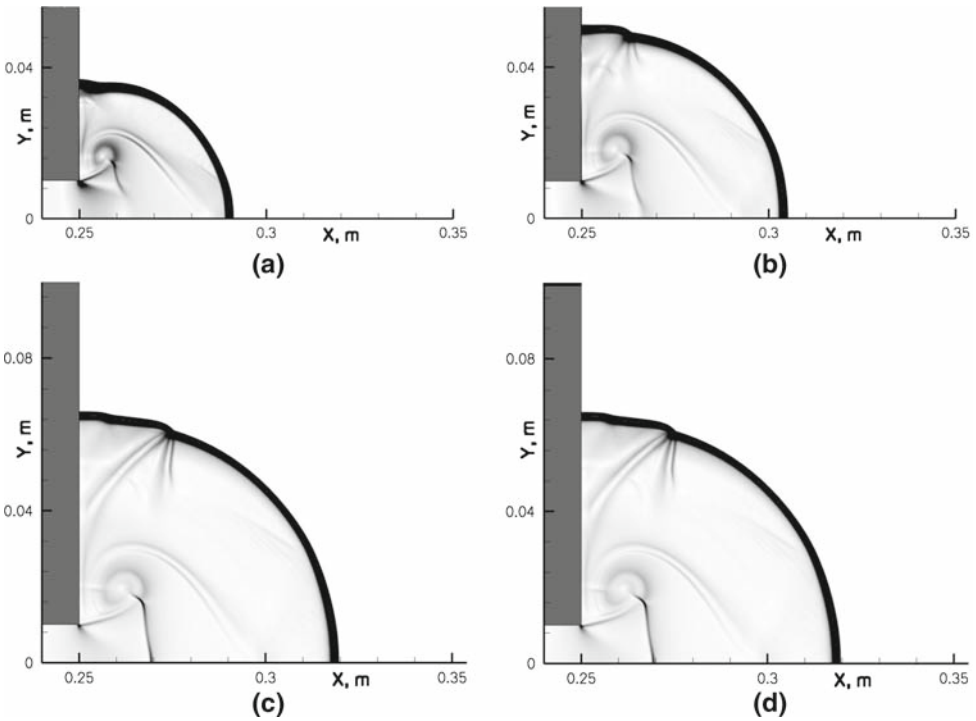

Fig. 6 Detonation behaviour in the supercritical regime, $d = 1\,\mu$m, $H1 = 0.01$ m, $t = 0.14$ ms (**a**); 0.15 ms (**b**); 0.16 ms (**c**); 0.18 ms (**d**)

corresponding to a gas flow with an adiabatic exponent γ_e corresponding to the equilibrium value of the mixture.

5 Detonation diffraction in gas–particle mixture

Three different scenarios of gaseous detonation wave propagation and diffraction on a backward-facing step are observed experimentally and described theoretically in [7–9]. A continuous propagation of the detonation front is possible (the supercritical propagation regime); a complete detonation failure (the subcritical regime) may also occur, as well as a partial detonation failure with a subsequent re-initiation (the critical regime). Transition from one regime to another in the same gaseous mixture depends upon channel geometry. In heterogeneous detonation of a gas–particle mixture, the combustion zone scale is determined by the particle size. Additionally, there are velocity and thermal relaxation zones for phases in shock-wave and detonation structures. Therefore, the particles size may also affect the regime boundaries.

The problem of detonation wave diffraction on a backward-facing step in the gas–particle mixture was studied for a stoichiometric mixture of aluminum particles in oxygen with particle diameter 1 μm, 2 μm, 3.5 μm. The channel width H_1 was varied from 0.01 m to 0.03 m.

Computations show that three regimes similar to these observed for gaseous detonations [9] are also possible in the gas–particle mixture: a regime with a complete detonation failure, with a partial failure, and with a continuous detonation propagation. Examples of detonation structures for each regime are presented in Fig. 6 (the supercritical regime), Fig. 7 (the subcritical regime), and Fig. 8 (the critical regime). Numerical schlieren images constructed from gas density gradients are shown for several times.

The detonation wave structure in a gas–particle mixture includes the leading SW, zones of velocity and thermal relaxation of phases, and a combustion zone. For continuous detonation propagation, the width of the detonation front structure does not change with time (although it depends on the particle size). For partial detonation failure (in critical regimes) or for complete detonation failure (in subcritical regimes), decoupling of the combustion front and the leading SW occurs. In the critical regime, decoupling only occurs over part of the front, on top in Fig. 8, until reinitiation. In the subcritical regime, decoupling of the combustion front from the leading SW occurs along the entire front and recoupling/reinitiation never takes place (Fig. 7).

As can be seen from the comparison of Figs. 6–8, the wave pattern in the neighborhood of the expansion angle is similar. Here also, the flow is similar to gaseous mixtures [9] since the particle concentration (remaining after combustion has ended) is very low. The general behavior in each regime is similar to gaseous detonation.

The formation of the primary transverse wave in critical regimes is also revealed in the diffracted wave interval (Fig. 6) as a consequence of a Mach configuration development near the wall. The appearance of secondary transverse

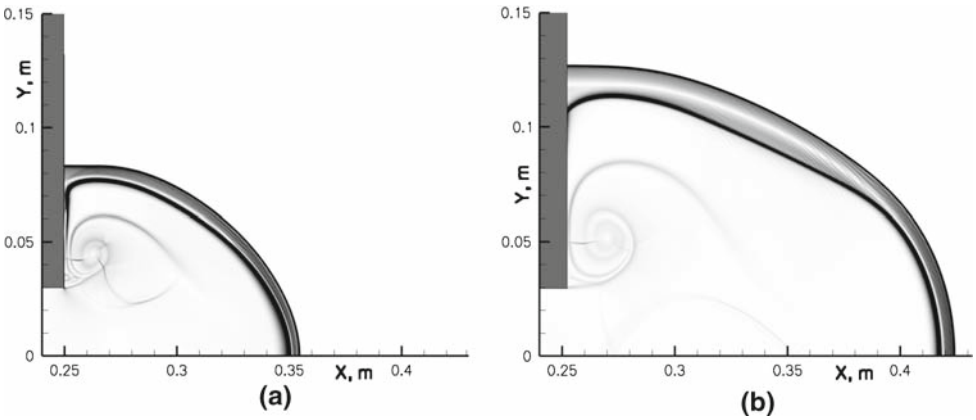

Fig. 7 Detonation failure (subcritical regime): $d = 3.5\,\mu$m; $H1 = 0.03$ m, $t = 0.19$ ms (**a**), 0.25 ms (**b**)

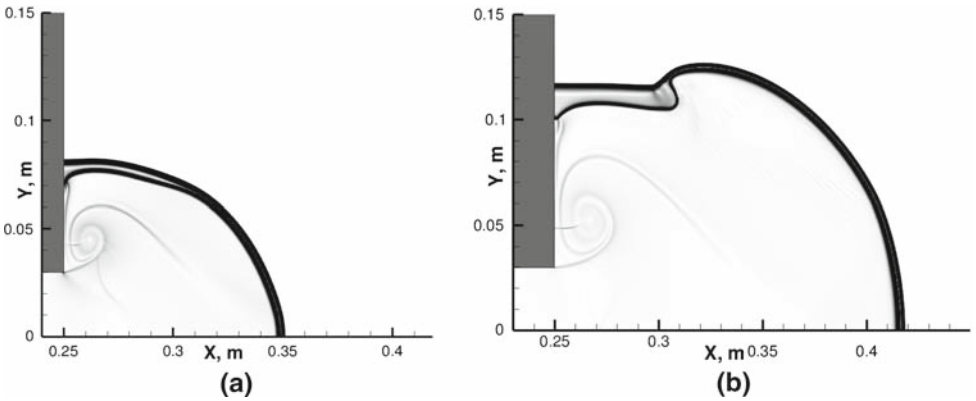

Fig. 8 Critical regime of detonation propagation: $d = 2\,\mu$m, $H1 = 0.03$ m, $t = 0.18$ ms (**a**), 0.23 ms (**b**)

waves related to propagation of disturbances in flow structure is discussed in [9]. Weak regular transverse waves (whose predecessors may be seen in Fig. 3d) also arise in the part of the front close to the symmetry plane, which lead to cellular detonation.

Decoupling between the leading front and the combustion front in subcritical regimes leads to shock-wave weakening and detonation failure.

In critical regimes, the wave front behind the expansion corner is divided into two parts: a detonation wave (in the neighborhood of the symmetry plane) and a shock decoupled from a lagging combustion front (close to the lateral wall). The wave propagation in the transverse direction slows down, and the flow structure in the region behind the backward-facing step is similar to the subcritical case. The detonation part of the front expands, becomes convex, and part of it propagates towards the wall of the backward-facing step, through the region of unburnt mixture between the diffracted SW and the lagging combustion front. After this transverse wave reflects from the wall of the backward-facing step, the front propagation acquires supercritical features.

The differences in wave pattern of the detonation flow from gaseous detonation are clear and they are related to relaxation.

The flow patterns in the near-wall region behind the backward-facing step are different for mixtures with different particle sizes. This leads to differences in the combustion front formation. Figure 9 shows the instantaneous streamlines patterns for mixtures with different particle sizes, in which the contours of the leading edge of the combustion front (the contours of particle temperature $T_2 = T_{ign}$) are shown by thick lines. For particles with $d = 3.5\,\mu$m (Fig. 9a, $H_1 = 0.03$ m, the subcritical regime) the width of the detonation wave structure is comparable with the forming vortex size. Some gas and particle mixture which has not reached the ignition temperature is entrained in the vortex motion, in a backward direction, which leads to a bend in the combustion front along the backward-facing step wall. From comparison of Figs. 9a and 7, it is clear that the near-wall bend of the combustion front is preserved in further developments and leads to its stretching along the wall.

In the mixture with $d = 2\,\mu$m for $H_1 = 0.005$ m, the regime is also subcritical, but the flow pattern in the near-wall region is different. The vortex zone and the complex of the leading SW with an adhering relaxation and combustion zone develop here separately. The combustion front does not stretch along the wall but sets against it (Fig. 9b), although a small bend of the front forms. The contact discontinuity

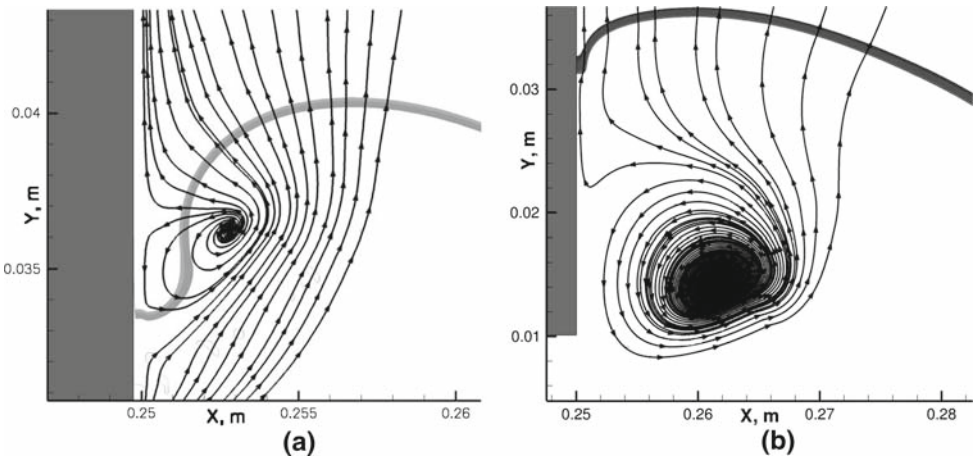

Fig. 9 Particles size influence on the wave pattern behind the backward-facing step. $d = 3.5$ MKM, $H1 = 0.03$ m, $t = 0.14$ ms (**a**); $d = 2\,\mu$m, $H1 = 0.005$ m, $t = 0.16$ ms (**b**)

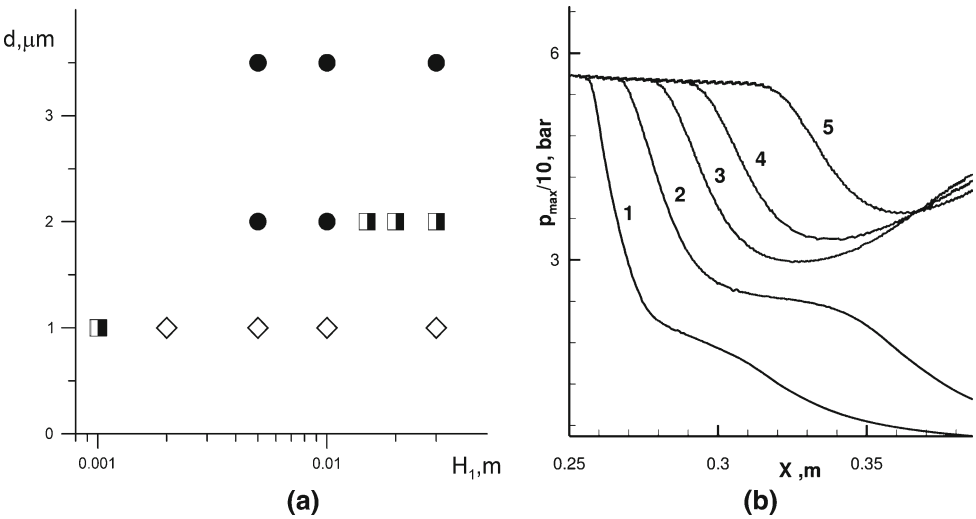

Fig. 10 Parameters influence on detonation propagation regime: detonation regime map (**a**); maximum pressure envelopes (**b**), $d = 2\,\mu$m, $H_1 = 0.005$ m (*curve* **1**), 0.01 m (**2**), 0.015 m (**3**), 0.02 m (**4**), $H1 = 0.03$ m (**5**)

adhering to the bend point of the combustion front, which can be seen in Fig. 8, represents what remains of a relaxation reflection of the near-wall wave (relaxation type of the SW reflection from a wall was noted in numerical computations in [26]).

The influence of particle size on transition from one regime to another is demonstrated in Fig. 10a, where a map of the regimes of detonation propagation is presented in the parameter plane of channel width and particle size. For each particle fraction there exists theoretically a range of channel widths corresponding to each regime. For example, for the gas–particle mixture of 1 μm, the critical regime is identified in numerical computations for the channel width of 0.001 m, for 2 μm at the channel width of 0.015 m. Figure 10b shows the envelope curves of the maximum pressure in the symmetry plane. Curves 1–2 correspond to detonation failure, and curves 3–5, to detonation preservation. A temporary detonation failure due to interaction with the expansion fan emanating from the corner manifests itself as a temporary reduction of the peak pressure on curves 3–5. Subsequent growth signals a re-initiation of the detonation wave. It can be concluded from analysis of our results that the propagation regime is determined by the ratio between geometric scales and relaxation scales (velocity, thermal, and chemical relaxation) that result from particle size.

Thus, detonations in gas–particle mixtures exiting from a channel into ambient space differs from the same process in gaseous mixtures because two factors. First, mixture dispersion affects the propagation regime. Second, the flow structure behind the backward-facing step differs due to interphase interaction.

6 Conclusions

1. Shock wave propagation in a gas–particle mixture in a flat duct with a sudden change in cross-section has been investigated numerically using a physical and mathematical model of the mechanics of heterogeneous media based upon a two-velocity and two-temperature approximation.

- Overall, the flow structure in mixture following SW diffraction at the cross-section discontinuity has been found to be qualitatively similar to diffraction in gases. The presence of particles, however, affects the shape and dimensions of the flow structure.
- For particle mass concentration values of the order of 0.1 and higher, particles mass loading affects significantly the expansion fan shape, the flow between the diffracted SW front and the contact surface, and the flow in vortex zone.
- The influence of particle size on diffraction pattern is most pronounced in the time interval when the typical dimensions of the structures are comparable with the relaxation scales.

2. Detonation wave diffraction in gas–particle mixture on a backward-facing step at the exit of a planar channel were studied numerically. The following was established:

- As in gases, three regimes of detonation propagation are possible: subcritical (detonation failure), critical (partial failure with subsequent re-initiation), supercritical (continuous detonation propagation).
- Which regime will occur depends not only upon the channel width but also on particle size.
- Some of the differences in the flow structure behind a backward-facing step are related to the influence of relaxation processes. In particular, in subcritical regimes, the interaction of relaxation zones with the vortex zone at the expansion corner gives rise to various combustion front shapes in the region behind the backward-facing step.

Acknowledgments This work was supported by the Russian Foundation for Basic Research (grant 06-01-00299).

References

1. Skews, B.W.: The perturbated region behind a diffracting shock wave. J. Fluid Mech. **29**(4), 705–719 (1967). doi:10.1017/S0022112067001132
2. Hillier, R.: Computation of shock wave diffraction at a ninety degrees convex edge. Shock Waves **1**, 89–98 (1991). doi:10.1007/BF01414904
3. Abate, G., Shyy, W.: Dynamic structure of confined shocks undergoing sudden expansion. Prog. Aerosp. Sci. **38**, 23–42 (2002). doi:10.1016/S0376-0421(01)00016-1
4. Takayama, K., Inoue, O.: Shock wave diffraction over a 90 degree sharp corner. Shock Waves **1**, 301–312 (1991). doi:10.1007/BF01418886
5. Wang, B.Y., Wu, Q.S., Wang, C., Igra, O., Falcovitz, J.: Shock wave diffraction by a cavity filled with dusty gas. Shock Waves **11**, 7–14 (2001). doi:10.1007/PL00004061
6. Bedarev, I., Gosteev, Y., Fedorov, A.: Shock-wave-initiated lifting of particles from a cavity. J. Appl. Mech. Tech. Phys. **48**(1), 17–26 (2007). doi:10.1007/s10808-007-0004-0
7. Shepherd, J.E., Schultz, E., Akbar, R.: Detonation diffraction. In: Ball, G., Hillier, R., Roberts, G. (eds.) Proceedings of the 22nd International Symposium on Shock Waves, vol. 1, pp. 41– 48 (2000)
8. Pantow, E.G., Fischer, M., Kratzel, T.: Decoupling and recoupling of detonation waves associated with sudden expansion. Shock Waves **6**, 131–137 (1996). doi:10.1007/BF02510993
9. Arienti, M., Shepherd, J.E.: A numerical study of detonation diffraction. J. Fluid Mech. **529**, 117–146 (2005). doi:10.1017/S0022112005003319
10. Kutushev, A.G., Shorokhova, L.V.: Numerical investigation of the processes of combustion and detonation of air-fuel mixtures of unitary fuel in abruptly expanding pipes. Chem. Phys. **22**(8), 94–99 (2003)
11. Kapila, A.K., Schwendeman, D.W., Bdzil, J.B., Henshaw, W.D.: A Study of Detonation Diffraction in the Ignition-and-Growth Model. Combust. Theory Model. No. **11**, 781–822 (2007). doi:10.1080/13647830701235774
12. Medvedev, A.E., Fedorov, A.V., Fomin, V.M.: Description of ignition and combustion of gas mixtures with solid particles by methods of the mechanics of continuous media. Combust. Expl. Shock Waves **20**(2), 127–132 (1984). doi:10.1007/BF00751577
13. Fedorov, A.V.: Structure of heterogeneous detonation of aluminum particles dispersed in oxygen. Combust. Expl. Shock Waves **28**(3), 277–286 (1992). doi:10.1007/BF00749644
14. Strauss, W.A.: Investigation of the detonation of aluminum powder-oxygen mixtures. AIAA J. **6**(12), 1753–1761 (1968). doi:10.2514/3.4855
15. Dreizin, E.L.: On the mechanism of asymmetric aluminum particle combustion. Combust. Flame **117**, 841–850 (1999). doi:10.1016/S0010-2180(98)00125-4
16. Beckstead, M.W.: Correlating Aluminum burning times. Combust. Expl. Shock Waves **41**(5), 487–495 (2005). doi:10.1007/s10573-005-0061-8
17. Borisov, A.A., Khasainov, B.A., Veyssiere, B., Saneev, E.L., Fomin, I.B., Khomik, S.V.: On detonation of aluminum dusts in air and oxygen. Sov. J. Chem. Phys. **102**, 369–402 (1992)
18. Fedorov, A.V., Khmel, T.A., Fomin, V.M.: Non-equilibrium model of steady detonations in aluminum particles—oxygen suspensions. Shock Waves **9**, 313–318 (1999). doi:10.1007/s001930050191
19. Fedorov, A.V., Khmel, T.A.: Numerical simulation of formation of cellular heterogeneous detonation of aluminum particles in oxygen. Combust. Expl. Shock Waves **41**(4), 435–448 (2005). doi:10.1007/s10573-005-0054-7
20. Fedorov, A.V., Khmel, T.A.: Numerical Simulation of Detonation Initiation With a Shock Wave Entering a Cloud of Aluminum Particles. Combust. Expl. Shock Waves **38**(1), 101–108 (2002)
21. Boiko, V.M., Kiselev, V.P., Kiselev, S.P., Papyrin, A.N., Poplavsky, S.V., Fomin, V.M.: Shock wave interaction with a cloud of particles. Shock Waves **7**, 275–286 (1997). doi:10.1007/s001930050082
22. Henderson, C.B.: Drag coeffcient of spheres in continuum and rarefied flows. AIAA J. **14**(6), 707–708 (1976). doi:10.2514/3.61409
23. Khmel, T.A.: Numerical simulation of two-dimensional detonation flows in reactive particle gas suspensions. Matematicheskoe modelirovanie **16**(6), 73–77 (2004) (in Russian)
24. Fedorov, A.V., Khmel, T.A.: Numerical technologies for investigations of heterogeneous detonations of gas particle suspensions. Matematicheskoe modelirovanie **18**(8), 49–63 (2006) (in Russian)
25. Khmel', T.A., Fedorov, A.V.: Interaction of a shock wave with a cloud of aluminum particles in a channel. Combust. Expl. Shock Waves **38**(2), 206–214 (2002). doi:10.1023/A:1014959117291
26. Fedorov, A.V., Kharlamova, Y.V., Khmel', T.A.: Reflection of a shock wave in a dusty cloud. Combust. Expl. Shock Waves **43**(1), 104–113 (2007). doi:10.1007/s10573-007-0015-4